

Parametric studies in friction stir welding on Al-Mg alloy with (HCHCr) tool by Taguchi based desirability function analysis (DFA)

C. Chanakyan^{a,*} and S. Sivasankar^b

^aResearch Scholar, Department of Mechanical Engineering, Government College of Engineering, Thanjavur, Tamilnadu, India

^bAssistant professor, Department of Mechanical Engineering, Government College of Engineering, Thanjavur, Tamilnadu, India

The present investigation is to optimize the welding parameters designed for friction stir welding (FSW) of aluminium magnesium alloy (AA5052). The authentic configuration of automated linear friction stir welding machine used to weld the AA5052. The experiments were conducted by selecting the different welding process parameters like tool rotation speed (rpm), traverse speed (mm/min), and tool pin profiles. The pin profile made with ceramic tool type (high carbon high chromium). Taguchi based desirability function analysis engaged in establishing the optimal process parameters with multi-objective function in order to maximize the tensile strength and the nugget hardness. The welding parameter of optimum level was attained by the highest composite desirability value. An optimal level of welding parameters acquired the tool rotation speed at 1200 rpm, traverse speed at 30 mm/min, and the pentagonal tool pin profile. Further, ANOVA (analysis of variance) implemented to intimate the major impact of welding parameters on the output responses (tensile strength and nugget hardness). An outcome perceived that the tool pin profiles and tool rotational speed are the important consequence factors to manipulate the mixed output responses. Contour plots and mean effect show that the interaction of parameters of welding on the required output response.

Keywords: DFA, HCHCr tool, FSW, Tensile, Microhardness, Microstructure.

Introduction

In the fusion welding process, the joining of aluminium alloy was inflexible, and blemish joints occurred due to a low melting point and high shrinkage. The welding institute introduced Friction stir welding (FSW) to solve this issues in the fusion welding process. There are many benefits in FSW such as, better mechanical properties, fine grain structure, free porosity, and extending the enormous amount of production in the automotive and marine sectors [1]. For setting the optimal level of welding process parameters, it is indispensable to produce the exceptional quality of the welding. There are different methods available to detect the optimal parameters of welding in which Desirability function analysis (DFA) is found as a precise method because it is less time consuming and materials for this current investigation [2]. Periyasamy et al. [3] reported the multi-objective optimization of FSW on the metal matrix composites by using the desirability function. The optimum process parameters of welding were achieved by desirability function to improve the responses of tensile strength, hardness, and notch strength. Ambedkar et al. [4] examined the process parameters of FSW multi-response by the

approach of principal component analysis and artificial neural network. They conducted the experiments on AA2024 aluminium alloy by utilizing the friction stir welding. These approaches considered the control factors as weld speed, tool rotation speed, and the tool dimensions ratio. They determined 3 D/d ratio, 670 r/min spinning speed of tool, and 0.017 m/min weld rate of optimal parameters by using principal component analysis. Devaiah et al. [5] summarized the dissimilar FSW between the AA5083 and AA6061 to attain the optimal welding parameters by utilizing the Taguchi. The most influencing parameters of weld rate and spinning speed of tool was indicated by the ANOVA outcomes and statistical model to create the correlation among the input variable and the result responses. The Taguchi technique produced the optimal parameters such as 1,120 rpm rotation speed of tool, 70 mm/min traverse speed, and 20° tilt angle from the multi-objective optimization. Devarasiddappa et al. [6] discussed the optimization of multi-objective in the WEDM process of the material Inconel 825 which composed by desirability function. The composite desirability produced the pulse off time for significant impact compared to other parameters namely peak current and pulse on time. The output responses namely surface roughness-SR and material removal rate-MRR with percentage of 3.73, 1.22, and 4.46, respectively. Jenarthan et al. [7] studied the impact of friction stir dissimilar welding between the AA2014 and AA6061 to develop the

*Corresponding author:
Tel : +91 9786964398
E-mail: chanmech89@gmail.com

tensile strength coupled with ANOVA and response surface methodology. They fabricated the high strength welding by using the control parameters such as weld speed, tool spinning, and the diameter of the tool pin. The CCD model validated by the ANOVA and also examines the mechanical response. John et al. [8] investigated the friction stir processing on AA2014 for developing the mechanical properties by the optimization and manipulate of input parameters. By an approach of desirability based response surface methodology to optimize the parameters of welding. The main objective of this examination was to find the optimal tool pin profile with an approach of desirability function. Kumar et al. [9] predicted and developed the tensile strength with the mathematical model for dissimilar FSW between the aluminium alloy 6061 and 2024 by ANN and Taguchi. At the 2nd level of processing parameters, the optimum value of the tensile strength of 189.1 MPa was obtained. The model results confirmed with an artificial neural network produce precise tensile strength compared to the Taguchi method. The good welded joint between the aluminium alloy 6061 and 2024 was produced with significant control parameters like weld rate, tool spinning rate, and axial load. Shashi Kumar et al. [10] identified the optimal process parameters of FSW on the 316 L material for maximizing the tensile strength by RSM based Box-Behnken design. The regression model established the response of tensile strength of the joint as an input factor such as spindle rate, weld rate, and axial load of tool. Those input factors significantly proved by the response surface method and desirability approach. Further, optimal outcomes of tensile strength 604 MPa corresponding to optimum input process parameters followed 597 rpm tool spindle speed, 74 mm/min tool weld speed, and 3 kN downward force. Kumar Naik et al. [11] proved that the optimization and investigation of Hardox 400 plasma arc cutting by desirability analysis based on the Taguchi method. To improve the quality of plasma arc cutting, Taguchi based desirability analysis-TBDA is utilized to obtain the optimal condition of cutting parameters. The plasma arc cutting efficiency was enhanced by setting optimal process parameters, which was verified by the confirmation test. Muthu Krishnan et al. [12] investigated the statistical modelling for the FSW of A319 and AA6063 using the ANN and response surface method. They proved that the welding process parameters like welding tool, tool spindle speed, axial force and traverse speed play an influential function in deciding the properties of the welded joints. The method ANN predicted the tensile strength of AA6063 and A319 FSW. The ANN regression model found the error in predicted values which was best technique in ANN compared to other ANN techniques. Nwobi-Okoye et al. [13] compared the modeling between artificial neural network and neuro-fuzzy system for multi-objective optimization of age hardening on A356

aluminium alloy. The neuro-fuzzy system with a coefficient 99.8% was the predicted hardness values which are finer than the artificial neural network having coefficient 99.2%. So that outside experimental points of ANN, which were the fitness functions of age hardening parameters using the (GA) genetic algorithm. Banglong Fu et al. [14] reported that the dissimilar friction stir welded joints between the AZ31B and AA6061 alloy. The transitional combination of rate of tool rotation 600rpm to 800rpm, the cross speed 30 mm/min to 60 mm/min and tool offset 0.3mm to obtain the welding. The eutectic structure survived in the nugget zone due to the intermetallics compounds of base metal. The tensile strength of the dissimilar joint reached 70% of AZ31B base metal. The spindle torque used to compute the heat-input between the base metal of AZ31B and AA6061 throughout the FSW process. The selected welding condition composed of the proper heat input and material mixing, which was studied in this investigation. Arun Kumar Kadian et al. [15] studied the material flow movement between the dissimilar AA 6061 aluminium alloy and B370 copper alloy through the friction stir welding. The material flow for the dissimilar FSW on the base material has been projected and located on the strain rate and temperature distribution. The temperature distributions were irregular in the welded samples because of the enormous amount of heat transmitted in copper material than the aluminium material. By maximizing the tool spinning speed, the material movement in welded plates can be improved. During the corrosion test, the volume of the fluid level was lower in the nugget region of the copper alloy due to lesser fluidity at the higher welding temperature. Palani K. et al. [16] conducted the dissimilar FSW on AA 8011 and AA 6061 al alloys. The three different tool pin profiles, such as hexagonal, pentagonal, and square, were played an essential role in promoting mechanical behavior during the welding process. The 1,500 rpm spinning speed of the tool, 40 mm/min traverse speed, and 2.5 mm depth of plunge with the hexagonal pin profile composed the excellent mechanical properties of dissimilar welded joints. Next to hexagonal pin profile, pentagonal pin produced defect-free AA 8011 and AA 6061 al alloy welded joints. Prabhakar et al. [17] investigated the FSP along with composite material of 5083 aluminium alloy and its reinforcement of fly ash particles. The FSP was fabricated at tool speeds 1,400 rpm, and varying weld speed of 20 and 25 mm/min which was concluded as the optimal condition. The maximum hardness attained in processed composite specimens when compared with base metal 5083. The current density of corrosion was maximized with processed 5083 aluminium alloy. The Al 5083 composites of processed specimens accomplished the fine grain size due to the presence of fly ash particles. Successfully, the researchers improved the performance of mechanical characteristics of processed composite 5083 aluminium

alloy. Gopi Krishnan et al. [18] had undergone the stir casting method with aluminium oxide and silicon carbide to produce the welded joints of AA7010. The working parameters, namely, axial force, traverse speed, and tool spinning speed, were varied. The welding parameter was designed with the L27 Taguchi technique. This investigation focused on the development of welded tensile strength by using regression analysis. The optimized parameters were done by the method of the Genetic algorithm.

In the present investigation, Taguchi based desirability function analysis implemented to determine the optimal process parameters for the Friction Stir Welded joints of AA5052, which was performed by ceramic tool material. There are several strengthening tool materials, namely, HSS, die steel, etc. Among these tool materials, high carbon high chromium (HCHCr) is a ceramic tool that possesses better strength for treating the surface of metals to improve the metallic characteristics in aluminium alloy. Moreover, ANOVA implemented to resolve the most critical impact of concerned parameters for the multiple responses, namely, tensile strength and nugget hardness. At last, the optimum process parameters confirmed by performing the verification test.

Materials and Methods

In this investigation, the friction stir welding of AA5052 was fabricated in FSW machine. AA5052 was good selection for integrated among aluminium alloys due to fine weldability, wear resistance, better corrosion, and superior hardness. Chemical composition and properties of the AA5052 base showed in Tables 1 and 2, correspondingly. HCHCr (High Carbon High Chromium Die Steel) utilized to manufacture the FSW tool. Fabricated tool pin profiles such as a Pentagonal pin cylinder (PC), straight cylinder (SC), and fluted cylinder (FC) displayed in Fig. 1. Aluminium alloy AA 5052 plates were having dimensions (100 mm × 50 mm × 6 mm), which are the required size of both specimen [19]. Square butt joint designed with size of 100 mm × 100 mm and equipped with welded joints. In the framework of single-pass welding, the welded joint was created. The revolving direction was typical for the welding direction with constant axial load of 5 kN was applied for all the experimentation.

Fig. 2 exhibits the photographic view of friction stir welded joints of AA5052. During the investigation, influence of tensile strength and nugget hardness of FSW on various welding parameters were examined. In present examination, the impacts of process parameters of welding with 3-levels were chosen and

it's given in Table 3. The L₉ orthogonal array selected for investigational outline of friction stir welding [20]. Tensile strength verified by the UTM-universal testing machine as per the standard of ASTM E9 used to prepare the tensile specimens. The microhardness analyzer with 0.5 N loads used to calculate the nugget hardness at three various spots for each nugget zone surface of welded specimen and the nugget hardness average value was measured. Investigational input process parameters of FSW and the outputs were exhibited in Table 4. Similarly, the photographic view of fractured

Table 2. AA 5052 Mechanical properties.

Tensile strength (MPa)	% of elongation	Microhardness (Hv)
251	19	70

Table 3. FSW process Parameters and its level.

Process Parameter	Notation	Level of factors		
		1	2	3
Tool rotational speed- (rpm)	RS-A	800	1000	1200
Traverse speed- (mm/min)	TS-B	20	25	30
Different profile of tool pins	TPP-C	SC	PC	FC



Fig. 1. The fabricated FSW tool pin profiles

Table 4. Effect on input process parameters on output responses with L₉ design.

Runs	Rotational Speed-RS	Traverse speed-TS	Tool pin profiles-TPP	Tensile Strength (MPa)	Nugget Hardness (Hv)
1	800	20	SC	190	60
2	800	25	PC	179	61
3	800	30	FC	188	63
4	1000	20	PC	180	69
5	1000	25	FC	187	68
6	1000	30	SC	174	67
7	1200	20	FC	185	66
8	1200	25	SC	170	63
9	1200	30	PC	191	67

Table 1. AA 5052 chemical composition.

Portion	Al	Mg	Fe	Zn	Cr	Mn	Si	Cu
Weight in %	Bal	2.5	0.3	0.2	0.2	0.1	0.1	0



Fig. 2. Friction stir welded joints of AA5052.



Fig. 3. Fractured tensile specimen of FSWed AA5052.

tensile specimen displayed in Fig. 3.

Result and Discussion

Desirability Function Analysis (DFA)

Derringer and Suich proposed the Desirability function analysis on optimizing multi-objective attributes conditions [21]. DFA utilized to transform multiple-response attributes interested in single response attributes among

the composite desirability inspection [22]. In present experimentation, the multiple responses namely tensile strength and nugget hardness mixed as composite desirability method. The following steps of DFA presented below:

Step (1): For all results of responses should be calculated by the individual desirability index (d_i). Three equations utilized to determine the index of

individual desirability [23].

Larger-the-better found to be the target for maximum objective function by using the following equation.

$$d_i = \begin{cases} 1, & \widehat{X} \leq X_{\min} \\ \left(\frac{\widehat{X}_j - X_{\max}}{X_{\min} - X_{\max}}\right)^r, & X_{\min} \leq \widehat{X}_j \leq X_{\max}, r \geq 0 \\ 0, & \widehat{X} \geq X_{\max} \end{cases}$$

Nominal-the-best found to be a goal for appropriate objective function by using the following equation.

$$d_i = \begin{cases} \left(\frac{\widehat{X} - X_{\min}}{T - X_{\min}}\right)^s, & X_{\min} \leq \widehat{X} \leq T, s \geq 0 \\ \left(\frac{\widehat{X} - X_{\max}}{T - X_{\max}}\right)^r, & T \leq \widehat{X} \leq X_{\max}, t \geq 0 \\ 0, & \text{Otherwise} \end{cases}$$

Smaller-the-better found to be a goal for minimum objective function by using the following equation.

$$d_i = \begin{cases} 1, & \widehat{X} \leq X_{\min} \\ \left(\frac{\widehat{X}_j - X_{\min}}{X_{\min} - X_{\max}}\right)^r, & X_{\min} \leq \widehat{X}_j \leq X_{\max}, r \geq 0 \\ 0, & \widehat{X} \geq X_{\max} \end{cases}$$

Here, X_{\max} is the greatest value of 'X', X_{\min} is the lowest amount of 'Y'. T- Signifies target values. The weight of the responses results was denoted by s, t, r. In the current investigation, tensile strength and nugget hardness were measured while the larger-the-better attributes.

Step (2): The individual desirability index of all responses are combined and used to determine the (d_G) composite desirability by subsequent equation.

$$d_G = \sqrt[w]{d_1^{w_1} * d_2^{w_2} * \dots * d_i^{w_i}}$$

Here, d_i denotes the individual desirability index along with w_i signifies weight of the output response.

Step (3): Once obtaining the composite desirability results, the optimal combination of the parameter level was measured. Commonly, composite desirability maximum value measured towards the optimum level of process parameters. Manipulated composite desirability among rank order was presented in Table 5.

Fig. 4 exhibits the rank plots between the composite desirability and the nine experimental runs. The Fig. 4 observed the 9th experiments attains the maximum of composite desirability. In which the 9th experiments intimates a superior combination of optimum level of welding parameters tool rotation speed (1,200 rpm),

Table 5. Composite desirability and its rank order.

Runs	Individual desirability		Composite Desirability	Rank
	Tensile strength	Nugget Hardness		
1	0.9524	0.0000	0	8
2	0.4286	0.1111	0.2182	7
3	0.8571	0.3333	0.5345	5
4	0.4762	1.0000	0.6901	3
5	0.8095	0.8889	0.8483	2
6	0.1905	0.7778	0.3849	6
7	0.7143	0.6667	0.6901	3
8	0.0000	0.3333	0	8
9	1.0000	0.7778	0.8819	1

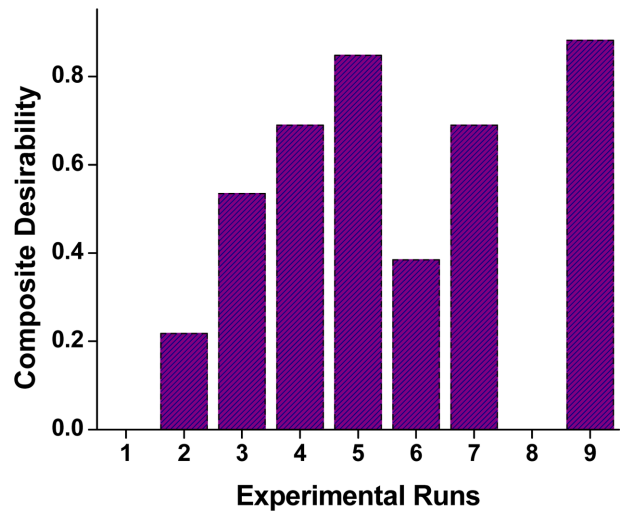


Fig. 4. The composite desirability vs the nine experimental runs.

tool traverse speed (30 mm/min), and pentagonal pin profile. Multi-response attributes to maximize the tensile strength and nugget hardness during the process of FSW on AA5052.

Analysis of FSW process parameters on composite desirability

Fig. 5 to 7 presented means of composite desirability with various FSW parameters. From the plots, the dotted line signifies the mean value of composite desirability. It is observed that the plots and the maximum value indicate the predicted characteristics of multiple responses. It indeed that the optimal level of FSW parameter arrangements obtained at the level $A_3B_3C_2$, which intimates that the tool rotation speed (1,200 rpm) at level 3, tool traverse speed (30 mm/min) at level 3, and tool pin profile (pentagonal cylinder) at level 2. Above the mentioned level of welding process parameters enhances the multi-responses of tensile strength and nugget hardness during the FSW process of AA5052 aluminium alloy. The mean and the average composite desirability for every process parameters level was displayed in Table 6. Therefore, table 6 clearly explains

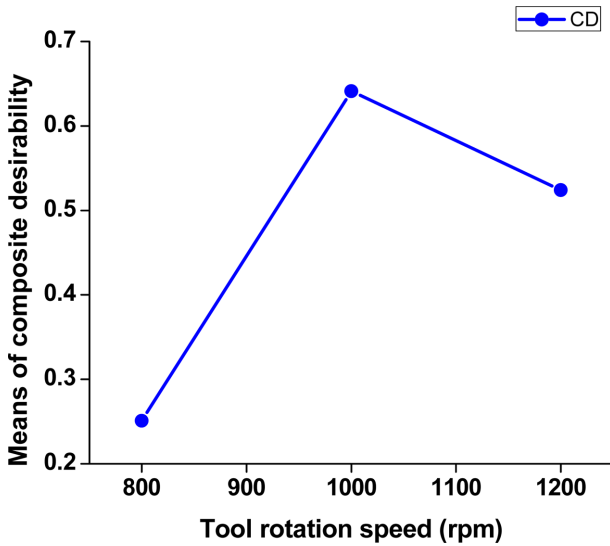


Fig. 5. Means of composite desirability vs Tool rotation speed.

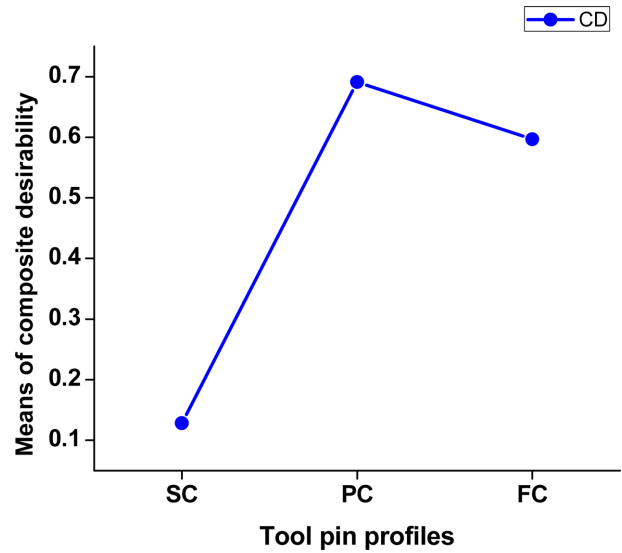


Fig. 7. Means of composite desirability vs Tool pin profiles.

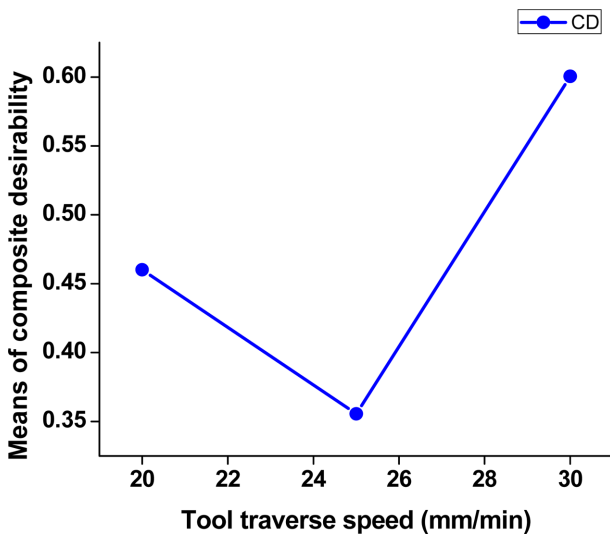


Fig. 6. Means of composite desirability vs Tool traverse speed.

Table 6. Composite desirability mean table.

Level	Tool rotation speed- (rpm)	Tool traverse speed- (mm/min)	Tool pin profile
1	0.2509	0.4601	0.1284
2	0.524	0.3555	0.691*
3	0.6411*	0.6004*	0.5967
Delta	0.3901	0.2449	0.5626
Rank	2	3	1

Average composite desirability = 0.471996

Table 7. Composite desirability ANOVA table.

Basis	(DOF)	(SS)	(MS)	F	P
Tool rotation speed	2	0.24048	0.12024	4.79	0.0323
Traverse speed	2	0.09062	0.04531	1.81	0.082
Tool Pin Profiles	2	0.54475	0.27238	10.86	0.021
Error	2	0.05016	0.02508		
Total	8	0.92600			

the order of control process parameters verified by the delta result. The highest delta value indicated as 1st rank, which denotes that, the control parameter which are the significant impact of output response. From mean table, the tool pin profile parameter was a significant aspect of the multiple performances of the developed welding process followed by the tool rotation speed.

Analysis of composite desirability

ANOVA objective is to manipulate the FSW parameters with contributions of integrated multi-response qualities [24]. Table 7 exhibited the ANOVA results of composite desirability. ANOVA results proved that the tool pin profile was the most influencing factor in which 62.1% contribution followed by tool rotation speed contributes 27.4%. The lowest contribution of 10.3% occurred in tool traverse speed. At a 95% confidence interval, the

significant process parameters were indicated by less than 0.05 of P-value. In this analysis, tool pin profiles ($p = 0.021$) and tool rotation speed ($p = 0.032$) severely affecting the process parameters on the output of multiple responses through the FSW of AA5052 [25].

Contour plot analysis for composite desirability

Fig. 8-10 exhibits the desirability contour plots with processing parameters of welding at different levels. In Fig. 8 showed, the impact of tool rate and tool traverse speed of composite desirability value. It is perceived that the value of composite desirability was increased while increasing the rate of tool rotation and weld speed. Maximum desirability value of 0.8820 was occurred at the tool rotation speed (1,200 rpm) and tool traverse speed (30 mm/min). In Fig. 9 showed that the effect of tool speed and three pin profiles of composite desirability value. It revealed that the tool rotation

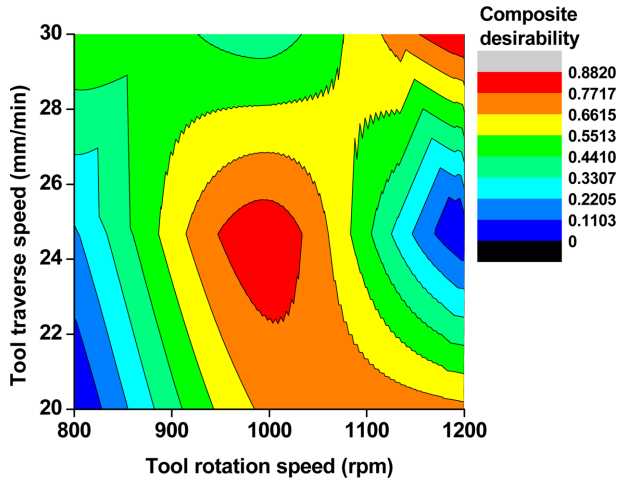


Fig. 8. Contour plot of composite desirability for Tool traverse speed vs Tool rotation speed.

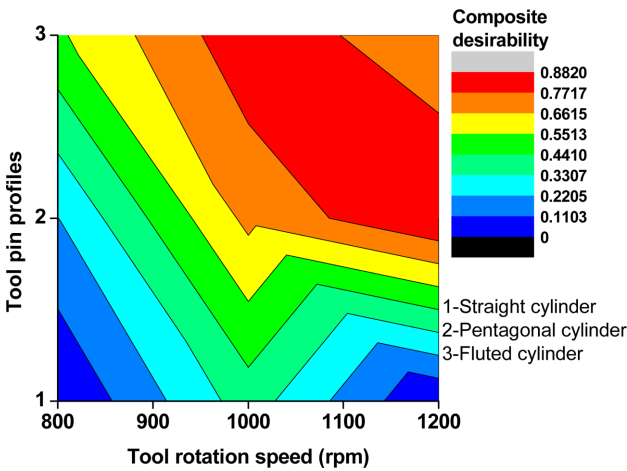


Fig. 9. Contour plot of composite desirability for Tool pin profiles vs Tool rotation speed.

speed (1,200 rpm) and pentagon pin profile produces the highest composite desirability value. Due to higher tool rotation produced higher friction between the base metal and the tool, thus the outcomes improved the tensile strength and nugget hardness. In Fig. 10 represents the response of tool traverse speed and tool pin profiles of the desirability values, the maximum value of composite desirability attained at the 30 mm/min tool traverse speed and pentagonal tool pin profile parameters.

Confirmation analysis of composite desirability

The verification test engaged to verify the investigational outcomes. An optimal level of FSW parameters utilized to validate the multi-response qualities during the process on AA5052. By using below the equation, the predicted value of composite desirability was determined.

$$\eta_{predicted} = \eta_m + \sum_{k=1} (\eta_i - \eta_m)$$

The composite desirability of average value and the

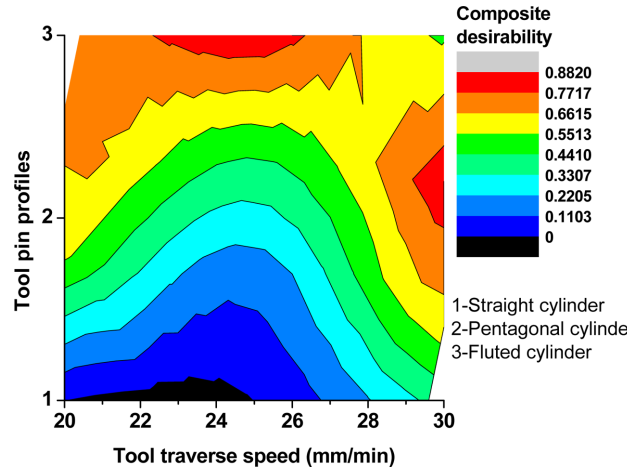


Fig. 10. Contour plot of composite desirability for Tool pin profiles vs Tool traverse speed.

Table 8. Confirmation analysis of experimented and predicted parameters.

Response parameters	Optimal Processing Parameters		
	Initial	Predicted	Experimental
Level of setting	A ₁ B ₂ C ₂	A ₃ B ₃ C ₂	A ₃ B ₃ C ₂
Tensile strength (Mpa)	179	191.9	191
Nugget hardness (Hv)	61	69	67
Composite desirability	0.282	0.9885	0.8819

Improved percentage of composite desirability = 68.02%

mean value indicated by η_m and η_i by the optimum level of process parameters. K-denotes the number of FSW parameters. Predicted, experimental and improved percentage on composite desirability value was presented in Table 8.

Microstructure

The optical microscopy investigation was conducted on the microstructure analysis of the entire AA5052 welded region with the influence of various welding parameters. The micrographs of stirred zone of joints were observed to dynamic recrystallization appeared during the welding. Also mentioned variations in grain size and homogeneity were determined in the welding technique [26]. The grain size was measured at three deformation zones, namely the nugget zone (NZ), thermo-mechanically affected zone (TMAZ), and heat-affected zone (HAZ). Heyn’s line intercept technique applied to determine the (AGD- Average Grain Diameter) of stirred zone on welded specimens. The granular grains of the base metal modified to fine grains in the nugget zone. The microstructure of fabricated FSW joints utilizing the optimum parameters were shown in Fig. 11. Mentioned figure shows the grain structure of friction stir welded at different zones with magnification of 100 × and 100 μm. In all the welded specimens, the nugget zone grain size is much smaller than the TMAZ and

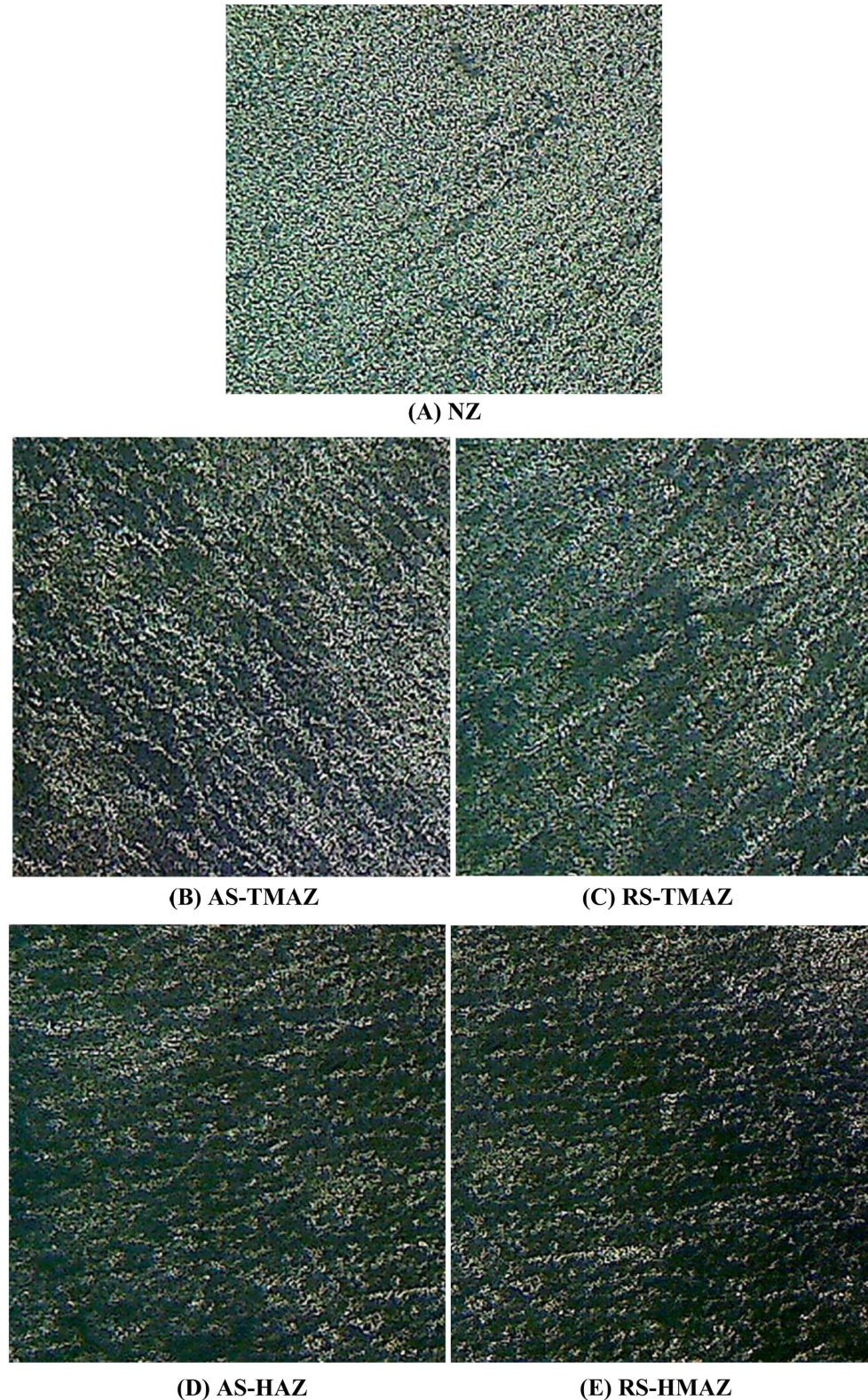


Fig. 11. Microstructure of different zones at the optimum process parameters 1,200 rpm, 30 mm/min and pentagonal cylinder tool .

HAZ. The advancing and retreating side of the TMAZ grain size is finer than that of the HAZ. The welded joints thermo mechanically affected zone – advancing side (TMAZ-AS) fabricated by the indicated process parameters exhibits coarse and elongated of deformed

grains at the welded interface. The welded joints thermomechanically affected zone - retreating side (TMAZ-RS) shows the elongated oriented grains due to the deformation of the welded interface was slowly reduced. The heat affected zone on advancing side (AS) and

retreating side (RS) micrographs show the coarsening of grain occurred in HAZ due to mechanically influenced deformation not occurred [27-29]. Fig. 11 presents the microstructures of various zones at the optimum process parameters with tool rotation speed (1,200 rpm), traverse speed (30 mm/min), and the pentagonal cylinder tool pin profile. The nugget zone grain size is much smaller than the TMAZ and HAZ. The advancing and retreating side of the TMAZ grain size is finer than that of the HAZ. The average grain diameter at the nugget zone is 1.59 μm .

Conclusion

1. The FSW of AA5052 aluminium alloy was effectively fabricated throughout this welding process and the optimal process parameters of FSW was investigated.
2. Taguchi based desirability function analysis was successfully employed to verify the optimum level of welding parameters during welding process.
3. The optimal level of process parameters are tool rotation speed (1,200 rpm), tool traverse speed (30 mm/min) and the pentagonal pin profile achieved maximum tensile strength and nugget hardness.
4. ANOVA outcomes showed, the tool pin profiles was the most significant factor for output responses with contribution of 62.1%. Subsequently, tool spinning rate and weld speed contributes the 27.4% and 10.3%.
5. The confirmation analysis of composite desirability utilized to validate the optimum level of process parameters so as to improve the composite desirability with 68.02%.

Acknowledgement

The authors express their genuine gratefulness to Coimbatore institute of technology (CIT), Coimbatore providing the amenities for conduct of the research.

References

1. T.A. Barnes and I.R. Pashby, *J. Mate. Proc. Tech.* 99[1-3] (2000) 62-71.
2. S.V. Alagarsamy, M. Ravichandran, S. Dinesh Kumar, S. Sakthivelu, M. Meignanamoorthy, and C. Chanakyan, *Mate. Today. Proc.* 27[2] (2020) 853-858.
3. P. Periyasamy, B. Mohan, V. Balasubramanian, S. Rajakumar, and S. Venugopal, *Tran. Nonf. Meta. Soci. Chin.* 23[4] (2013) 942-955.
4. M. Ambekar and J. Kittur, *Mate. Today. Proc.* 27[1] (2019) 363-368.
5. D. Devaiah, K. Kishore, and P. Laxminarayana, *Mate. Today. Proc.* 5[2] (2018) 4607-4614.
6. D. Devarasiddappa, M. Chandrasekaran, and M.T. Sambandam, *Mate. Today. Proc.* 5[5] (2018) 11531-11547.
7. M.P. Jenarthanam, C. Varun Varma, and V. Krishna Manohar, *Mate. Today. Proceedings* 5[6] (2018) 14384-14391.
8. J. John, S.P. Shanmuganatan, and M.B. Kiran, *Mate. Today. Proc.* 5[11] (2018) 25458-25467.
9. A. Kumar, M.K. Khurana, and G. Singh, *Mate. Toda Proc.* 5[11] (2018) 25440-25449.
10. S. Shashi Kumar, N. Murugan, and K.K. Ramachandran, *Measurement.* 137 (2019) 257-271.
11. D.K. Naik and K.P. Maity, *Mate. Today. Proc.* 5[5] (2018) 13157-13165.
12. M. Muthu Krishnan, J. Maniraj, R. Deepak, and K. Anganan, *Mate. Today. Proc.* 5[1] (2018) 716-723.
13. C.C. Nwobi-Okoye, B.Q. Ochieze, and S. Okiy, *J. Mate. Rese. Tech.* 8[3] (2019) 3054-3075.
14. B. Fu, G. Qin, F. Li, X. Meng, J. Zhang, and C. Wu, *J. Mate. Proc. Tech.* 218 (2015) 38-47.
15. A.K. Kadian and P. Biswas, *J. Manuf. Proc.* 34 (2018) 96-105.
16. K. Palani, C. Elanchezian, B. Vijaya Ramnath, G.B. Bhaskar, and E. Naveen, *Mate. Today. Proc.* 5[11] (2018) 24515-24524.
17. Prabhakar, N. Ravi Kumar, and B. Ratna Sunil, *Mate. Today. Proc.* 5[2] (2018) 8391-8397.
18. P. Gopi Krishnan, B. Suresh Babu, and K. Siva, *J. Ceram. Process. Res.* 21[2] (2020) 157-163.
19. C. Chanakyan and S. Sivasankar, *Inte. J. Rapi. Manu.* 8[1/2] (2019) 147-160.
20. C. Chanakyan and S. Sivasankar, M. Meignanamoorthy, M. Ravichandran, and T. Muralidharan, *Mate. Toda. Proc.* 21 (2020) 231-236.
21. B. Singaravel and T. Selvaraj, *J. Adva. Manu. Syst.* 15[1] (2016) 1-11.
22. M. P. Jenarthanam and R. Jeyapaul, *Inte. J. Scie. Tech.* 5[4] (2013) 23-36.
23. P. Sengottuvel, S. Satishkuma, and D. Dinakaran, *Proc. Engi.* 64 (2013) 1069-1078.
24. S.V. Alagarsamy and M. Ravichandran, *Indu. Lubr. Trib.* 71[9] (2019) 1064-1071.
25. R. Bobbili, V. Madhu, and A.K. Gogia, *Engi. Scie. Tech. Inter. J.* 18[4] (2015) 720-726.
26. G. Ugrasen, G. Bharath, G. Kishor Kumar, R. Sagar, P.R. Shivu, and R. Keshavamurthy, *Mate. Toda. Proc.* 5[1] (2018) 3027-3035.
27. K. Meena, A. Kumar, and S.N. Pandya, *Mate. Toda. Proc.* 4[2] (2017) 1978-1987.
28. H. Fujii, L. Cui, M. Maeda, and K. Nogi, *Mate. Scie. Engi. A.* 419[1-2] (2006) 25-31.
29. P. Thread Gill, *Science and Technology of Welding and Joining* 12[4] (2007) 357-360.